



Article

Influence of a Dynamic Consolidation Force on In Situ Consolidation Quality of Thermoplastic Composite Laminate

Berend Denkena ¹, Carsten Schmidt ² , Maximilian Kaczemirzk ^{2,*} and Max Schwinn ³

¹ Institute of Production Engineering and Machine Tools, Leibniz Universität Hannover, An der Universität 2, 30823 Garbsen, Germany; denkena@ifw.uni-hannover.de

² Institute of Production Engineering and Machine Tools, Leibniz Universität Hannover, Ottenbecker Damm 12, 21684 Stade, Germany; schmidt@ifw.uni-hannover.de

³ Institute of Polymer Materials and Plastics Engineering, Clausthal University of Technology, Ottenbecker Damm 12, 21684 Stade, Germany; max.schwinn@tu-clausthal.de

* Correspondence: kaczemirzk@ifw.uni-hannover.de; Tel.: +49-4141-77638-22

Abstract: For achieving high quality of in situ consolidation in thermoplastic Automated Fiber Placement, an approach is presented in this research work. The approach deals with the combination of material pre-heating and sub-ultrasonic vibration treatment. Therefore, this research work investigates the influence of frequency dependent consolidation pressure on the consolidation quality. A simplified experimental setup was developed that uses resistance electrical heating instead of the laser to establish the thermal consolidation condition in a universal testing machine. Consolidation experiments with frequencies up to 1 kHz were conducted. The manufactured specimens are examined using laser scanning microscopy to evaluate the bonding interface and differential scanning calorimetry to evaluate the degree of crystallinity. Additionally, the vibration-assisted specimens were compared to specimens manufactured with static consolidation pressure only. As a result of the experimental study, the interlaminar pore fraction and degree of compaction show a positive dependency to higher frequencies. The porosity decreases from 0.60% to 0.13% while the degree of compaction increases from 8.64% to 12.49% when increasing the vibration frequency up to 1 kHz. The differential scanning calorimetry experiments show that the crystallinity of the matrix is not affected by vibration-assisted consolidation.

Keywords: CFRP; thermoplastic; in situ consolidation; vibration; AFP



Citation: Denkena, B.; Schmidt, C.; Kaczemirzk, M.; Schwinn, M. Influence of a Dynamic Consolidation Force on In Situ Consolidation Quality of Thermoplastic Composite Laminate. *J. Compos. Sci.* **2021**, *5*, 88. <https://doi.org/10.3390/jcs5030088>

Academic Editor:
Francesco Tornabene

Received: 8 March 2021
Accepted: 18 March 2021
Published: 22 March 2021

Publisher's Note: MDPI stays neutral with regard to jurisdictional claims in published maps and institutional affiliations.



Copyright: © 2021 by the authors. Licensee MDPI, Basel, Switzerland. This article is an open access article distributed under the terms and conditions of the Creative Commons Attribution (CC BY) license (<https://creativecommons.org/licenses/by/4.0/>).

1. Introduction

Thermoplastic fiber-reinforced composites (TPC) are attracting increasing interest in the aviation industry due to their advantages, such as weldability, recyclability, chemical resistance and fracture toughness compared to thermoset materials [1–3]. One method to manufacture TPC structures is the processing of pre-impregnated tapes by Automated Fiber Placement (AFP) technology. This additive manufacturing process offers a high degree of automation as well as high repeat accuracy and, thus, offers a high potential for efficient production [2,4–6]. Due to the meltability of the thermoplastic matrix, the Thermoplastic Automated Fiber Placement (TAFP) process shows the potential to be carried out without a post-consolidation step. This potentially eliminates the need for the autoclave process and enables an out-of-autoclave composite manufacturing, so that high investment costs and running costs can be reduced. However, the difficulty with the in situ TAFP process is achieving a laminate quality that is equivalent to the autoclave process. Recent studies [7,8] show that the in situ quality in terms of mechanical laminate properties does not match the quality of composite parts from autoclave processes. For example, [7] shows that the interlaminar shear strength and the flexural properties are below the autoclave quality.

Hence, a special focus must be placed on the consolidation step at the nip-point. During the consolidation, the heated fed tape and the heated substrate are pressed together

by applying the consolidation pressure. Here, it is crucial that the largest possible contact area is formed between the tape surface and the substrate surface. This contact area is called intimate contact. Diffusion processes (autohesion) of polymer chains take place via this interface and thus bonding strength develops [3,9–13]. A larger contact area leads to better diffusion processes and thus to higher bond strength [3,9–16]. The formation of interlaminar pores or air pockets is synonymous with low intimate contact. In different studies it was found that the arising of high intimate contact is influenced by the surface of both the tape and the substrate, the consolidation time, the consolidation pressure and the temperature-dependent viscosity and thus the tape temperature [3,9,12,17]. Based on these findings, squeeze flow models for prediction of intimate contact have been developed. In special cases, these models showed a limited accuracy in comparison to experimental investigations [18–20]. For a precise prediction of intimate contact, other mechanisms, e.g., surface energy for low-viscosity PA-6 [20] or percolation flow for fiber-rich surfaces [15,21], must be considered extending the squeeze flow theory. However, all theories have in common that viscosity is a crucial factor which makes the need for precise temperature control within the nip-point essential.

Therefore, Laser-based TAFP systems (Figure 1) are used for in situ manufacturing TPC structures, since lasers offer energy-efficient heating as well as fast and precise control response. However, due to the large housing, the laser must be used at a certain angle to the substrate surface which leads to a shadow zone in front of the nip-point [4,7,8,15]. Depending on the flexibility of the consolidation roller (e.g., a rigid steel roller [9–14,18] or a flexible silicone roller [4,7,15,19,20,22–24]), a larger or smaller shadow zone arises. As a consequence, the nip point cannot be reached directly with the laser radiation, so both the tape and the substrate are only heated by reflected laser radiation [4,8,23] which leads to a temperature loss towards the nip point [18]. This drop in temperature can cause a sub-melt temperature at the nip-point and thus a high viscosity of the material which results in low intimate contact, high porosity and poor consolidation quality. The temperature loss can be compensated by heating the tape and the substrate in front of the shadow area above melting temperature [4,7,8]. Depending on the laying speed and the size of the shadow area, the temperature can rise up to 550 °C when processing carbon-fiber reinforced polyetheretherketon (PEEK/CF) [18]. Due to the fast overheating of the material near to the degradation temperature, fiber-rich surfaces can occur and thus time-consuming percolation must be considered for high intimate contact. A consequence of this degraded matrix material is a decrease in bonding strength [24–28]. Furthermore, due to the high temperature deconsolidation effects, e.g., void growth as a consequence of temperature-dependent gas expansion, are observable [29].

This research paper considers a novel approach to avoid the temperature loss related effects within laser-based in situ TAFP and thus to improve the development of intimate contact and consolidation quality. The approach proposes the excitation of the consolidation roller with sub-ultrasonic vibrations in addition to the laser heating in TAFP. Through this, the frequency-dependent shear-thinning effect of the viscoelastic matrix material will be used to decrease the viscosity within the consolidation as well as dissipative heat generation which is known from tape winding [30–32] and ultrasonic welding [33–35] of the thermoplastic material will be used to compensate the temperature loss and avoid overheating. Both the shear-thinning effect and dissipative heat effect shall have a positive effect on the development of intimate contact and thus on the resulting consolidation quality. While a vibration-excited end effector for implementation in TAFP is under development, this research work investigates in a preliminary study the influence of a dynamic force in combination with a pre-heated consolidation process on the formation of interlaminar pore content as well as the compaction behavior and crystallization.

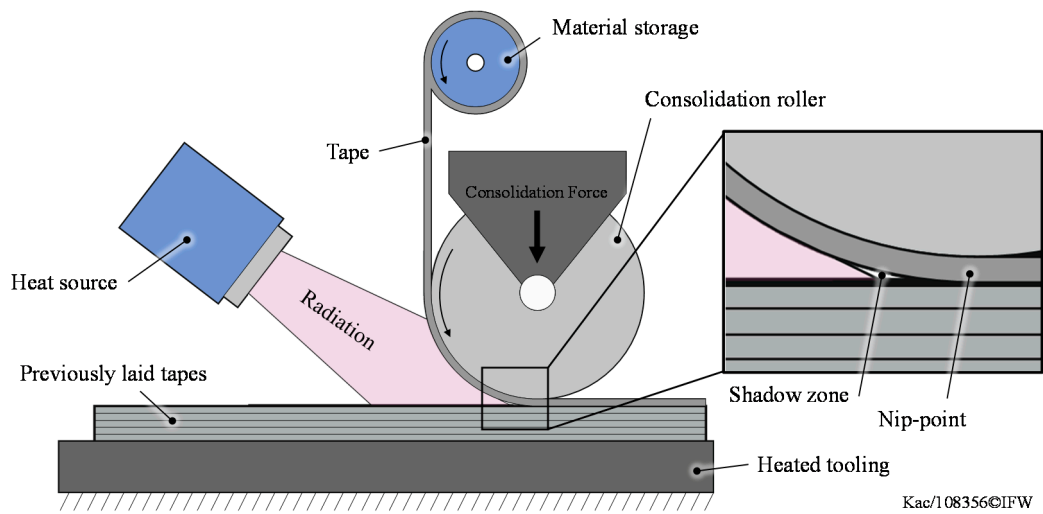


Figure 1. Schematic illustration of the laser-based Thermoplastic Automated Fiber Placement (TAFP) technology including the appearing shadow zone in front of the Nip-point.

2. Materials and Methods

2.1. Experimental Setup

For the preliminary experimental investigations, a test setup (Figure 2) was designed to simplify and transfer the AFP consolidation process into an INSTRON 8870 universal testing machine (Norwood, MA, USA) considering a stamp/tool system. The stamp has a flat area of 35 mm × 15 mm (length × width). With reference to the width of the prepreg tapes, double-layer unidirectional specimens with a size of 35 mm × 11.5 mm can be manufactured using this test setup.

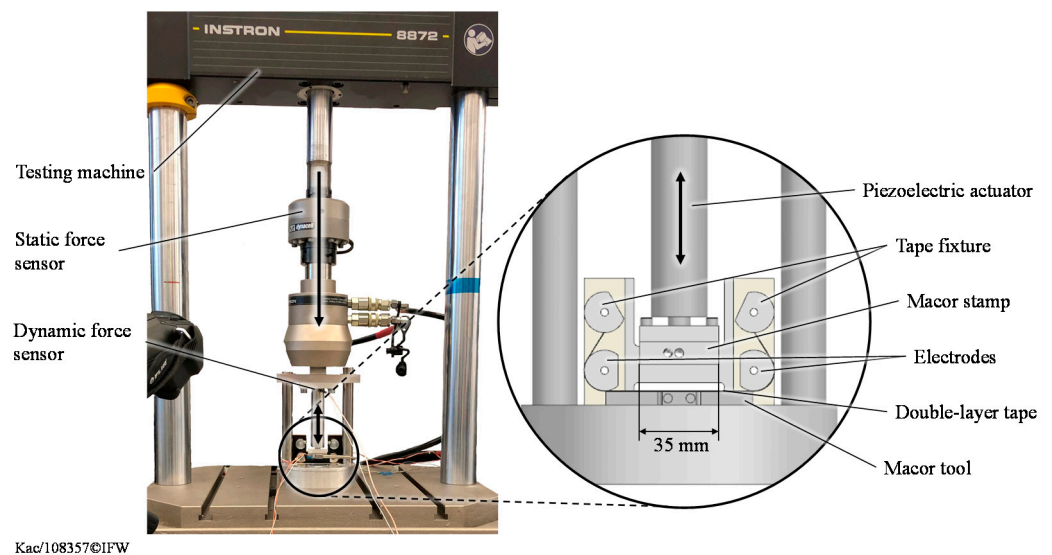


Figure 2. Test setup used for the consolidation experiments.

Since laser heating cannot be used within the universal testing machine due to safety restrictions, the heating of the specimens takes place via electrically conductive carbon fibers utilizing a temperature control module based on the effect of resistance electrical heating according to Joule’s principle. Uniform contact with the carbon fibers is relevant for homogeneous temperature control. The implementation of the contact is based on a combination of tensile and compressive force and is implemented by a multi-roller construction. The temperature is set via a power control on the power supply unit. A performance characteristic was developed with which a repeatable setting of the temperature can be

achieved. In order to prevent a temperature drop due to conductive heat flux from the hot tape into the stamp during the consolidation, the Macor glass ceramic is selected as the material for the stamp and tool. At $1.46 \text{ W/m}^2\text{K}$, the thermal conductivity of Macor is below the thermal conductivity of, e.g., steel ($50 \text{ W/m}^2\text{K}$). Thus, the heat flux is reduced and has a smaller influence on the consolidation temperature.

The static consolidation force is applied by the testing machine while the mechanical excitation of the consolidation stamp and thus the application of the dynamic force component takes place according to the inverse piezoelectric principle, in which a piezoelectric ceramic is mechanically stretched when an electrical field is applied. For this purpose, the piezoelectric linear actuator PSt 1000/16/100 VS25 with the control electronics HV-RCV-1000/3 (piezosystem jena, Jena, GER) is used in this experimental setup. The expansion of the actuator is proportional to the applied electric field strength and shows an almost linear increase in strain with the applied voltage in the operating range. The maximum elongation of $100 \mu\text{m}$ is achieved at a voltage of 1000 V . In relation to the initial length of the linear actuator of 107 mm , this corresponds to an elongation of 0.094% . The hysteresis effects that predominate in piezoelectric actuators can be neglected in the case of sinusoidal movements. In dynamic applications, the power electronics are decisive for the repeatability and accuracy of the movement. The used control electronics achieve a maximum operating frequency of 2.5 kHz for dynamic applications. The static consolidation force is measured by the INSTRON static force sensor. The vibrations are monitored with the single-axis force sensor SlimLine 9134B21 (Kistler, Winterthur, CHE) at a sampling rate of 6.25 kSp/s .

2.2. Material

PEEK/CF was selected for carrying out the experiments. The fiber weight fraction of the utilized PEEK/CF is $65 \text{ wt.}\%$ and the fiber volume content is $57 \text{ vol.}\%$. The processing pressure was specified as $20 \text{ bar} \pm 10 \text{ bar}$ and the process temperature as $380 \text{ }^\circ\text{C}$. The prepreg material is available as slit tape with a width of 11.5 mm . The origin thickness of the material is $160 \mu\text{m}$.

2.3. Specimen Manufacturing

When carrying out the experiments, two tapes were manufactured to a consolidation specimen. For this purpose, the PEEK tapes were cut to a length of 145 mm and provided with copper tape at the points of electrical contact to ensure homogeneous temperature control. The prepared samples were inserted into the temperature control module and heated to the required process temperature. When the process temperature is reached, the testing procedure of the universal testing machine starts and applies the required process pressure to the samples. As soon as the process pressure is reached, the mechanical excitation takes place via the piezoelectric actuator. After the set consolidation time has elapsed, the testing machine opens and the temperature control is stopped. The process parameters used to produce the different specimens are shown in Table 1.

Table 1. Processing parameters used in the consolidation experiment.

Specimen	Temperature $^\circ\text{C}$	Static Force N	Amplitude μm	Frequency Hz	Time s
Reference	380	650	10	0	3
F1	380	650	10	100	3
F2	380	650	10	500	3
F3	380	650	10	1000	3

2.4. Consolidation Quality Evaluation

2.4.1. Laser Scanning Microscopy

For the evaluation of the interlaminar pore content as well as the compaction of the specimens, cross-section samples were taken from the double-layer specimens and

analyzed microscopically. The laser confocal microscopy method according to EN ISO 25178-607 was used for these examinations. With this method two-dimensional geometrical analyses as well as three-dimensional determination of the pore content can be carried out. The microscopic examinations were carried out on a Keyence VK-X1000 (Osaka, JPN) surface profilometer.

To determine the compaction of the origin tape, cross-sectional images were taken with 240× and 480× magnification. The recording and processing of the image data were carried out with Keyence Multi-File-Analyzer[®] software. To determine the tape width w_{cons} after consolidation, the recordings were made with a 240× magnification. During the recording, the micrographs were automatically stitched to form an overall image. To determine the tape thickness t_{cons} after consolidation, the micrographs were analyzed as individual images with a 480× magnification. The thickness was evaluated at ten points on the samples, which were evenly distributed throughout the width of the tape. Based on the condition of the semi-finished product with a width of 11.5 mm and a tape thickness of 160 μm, or 320 μm for the double-layer specimen, the tape compaction was analyzed. For calculation of the degree of compaction (DC) with Equation (1), the cross-sectional areas (CSA) were formed from the tape width w_{cons} and the mean value of the tape thickness t_{cons} and expressed in relation to the initial area A of 3.68 mm² (11.5 mm × 0.32 mm).

$$\text{DC} = \frac{w_{\text{cons}} t_{\text{cons}}}{A} \quad (1)$$

The evaluation of the pore content is based on cross-sectional images with 1200× magnification. The multi-file analyzer software and the particle analysis module were used to determine the degree of porosity DP by relating the sum of the determined pore areas AP to the total image area A_{pic} according to Equation (2).

$$\text{DP} = \frac{\sum AP}{A_{\text{pic}}} \quad (2)$$

In order to differentiate the pores from other artifacts such as fiber fragments that arise during the grinding process, surface scans were used to separate the pores using a threshold algorithm. The threshold algorithm separates the pores from other artifacts based on their depth. For example, fiber breakouts have a depth of <1 μm, while pores have a depth of >>1 μm.

2.4.2. Differential Scanning Calorimetry (DSC)

The DSC experiments were conducted to evaluate the influence of vibrations on the degree of crystallization. Based on DIN EN ISO 11357, a Discovery DSC by TA Instruments (New Castle, DE, USA) and the associated software Trios were utilized to determine the degree of crystallization of consolidation specimens. The heating and cooling rate was set to 20 K/min and the maximum temperature amounted to 400 °C. An experiment consisted of two heating and one cooling sequence between 90 °C and 400 °C. After reaching the final temperature the temperature was kept isothermal for 5 min, while nitrogen as purging gas was used. The degree of crystallization k can be calculated with Equation (3).

$$k = \frac{\Delta h_{\text{m}} - \Delta h_{\text{c}}}{\Delta h_{\text{lit}}} \quad (3)$$

In this equation Δh_{m} is the enthalpy of fusion, Δh_{c} the enthalpy of recrystallization and Δh_{lit} the enthalpy of completely crystalline material. The h_{lit} is a theoretical value from the literature, it amounts 130 J/g [36] while the enthalpy of fusion Δh_{m} and the enthalpy of recrystallization Δh_{c} need to be determined experimentally.

3. Results

3.1. Consolidation Force

With regard to the relaxation kinetics of the neat thermoplastic matrix material that are related to the viscosity of the matrix material and the consolidation force, the evaluation of the change in consolidation force was conducted to evaluate a change in viscosity. A change in viscosity can be affected by both temperature and frequency. Considering the theoretical background, the influence of the temperature on the viscosity and the relaxation behavior is low after reaching the melting temperature [9,37,38] while the influence of the frequency on the viscosity of the molten material is higher [34]. That leads to the expectation that a loss in consolidation force during the consolidation process would be observable with regard to the excitation frequency of the consolidation stamp.

On the abscissa, Figure 3a shows the consolidation time while the ordinate shows the static consolidation force. Considering these consolidation force curves, a decrease in the static consolidation force with increasing frequency is observable. The consolidation force of the reference samples decreases by about 15 N over a consolidation time of 3.2 s, while the relaxation of force for the 100-Hz samples is about 30 N over the same period. With a frequency excitation of 500 Hz, there is a decrease in the consolidation force of 90 N after a consolidation time of 3.2 s. When excited at 1000 Hz, the absolute value of the decrease in consolidation force is the same as in the 500-Hz experiment. However, the 1000 Hz decrease is already reached after 2.25 s of consolidation time and remains at this level until the end of the consolidation time. Thus, a saturation of relaxation capacity is observable and the same level of decrease in consolidation force is reached about 1 s earlier at the 1000-Hz experiment. Another remarkable point is the loss of consolidation pressure due to the relaxation of the material. The initial consolidation pressure reduces from 16 bar to 15.7 bar (Reference), 15.4 bar (100 Hz) and 14 bar (500 and 1000 Hz). Considering the evaluation of the consolidation force, the expected decrease in consolidation force in dependency of the frequency is observable which means that it is possible to decrease the viscosity of the composite material during a pre-heated consolidation process. According to the intimate contact models [9–13] the decreasing viscosity must have a positive influence on the bonding quality while the reduction in consolidation pressure must have a negative influence. Furthermore, these experiments are conducted with a long consolidation time compared to typical AFP consolidation times that are at least a factor of 10 smaller. With regard to these AFP consolidation times the consolidation force curves with higher frequencies also show a higher relaxation capacity at the time directly after the beginning of consolidation but the absolute value of decrease in consolidation force is considerably lower compared to the absolute value after 3.2 s. To increase the relaxation capacity and the change in viscosity directly after beginning of the consolidation and thus make it suitable for use in laser-based TAFP higher frequencies must be considered.

3.2. Interlaminar Porosity and Compaction

Interlaminar pores are a crucial factor for the formation of intimate contact during the consolidation process and usually arise during lay-up process, while intralaminar pores are already present in the tape and expand further due to the influence of high temperature. The optical analysis is conducted to determine the influence of the raising frequencies on the formation of interlaminar pore content and the compaction behavior of the material. With regard to the results of static force evaluation as well as to the intimate contact models, only small effects are expected due to the positive influence of decrease in viscosity and the negative influence of the decrease in consolidation pressure.

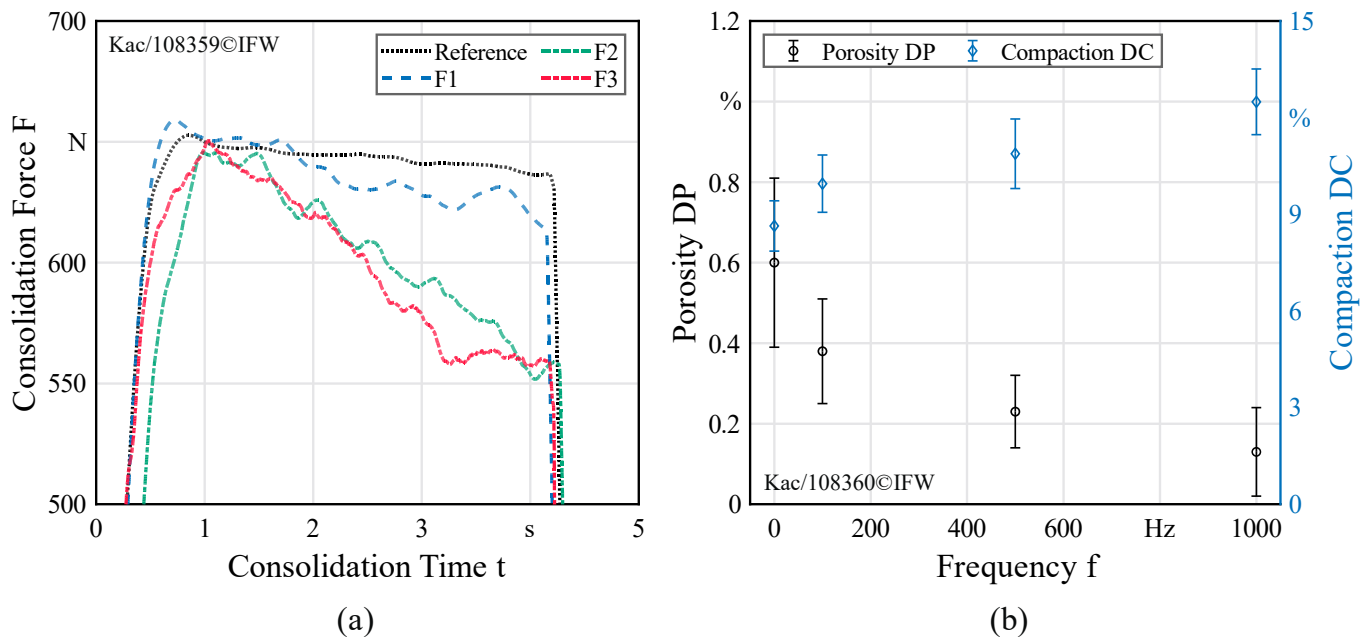


Figure 3. (a) Measured static consolidation force in relation to the consolidation time for the varied excitation frequencies; (b) Degree of Porosity (DP) and Degree of Compaction (DC) in relation to the varied excitation frequencies determined by Laser Scanning Microscopy.

Figure 3b shows the relation of the porosity and the compaction to the applied frequencies. The abscissa shows the investigated frequencies from 0 Hz (Reference) to 1000 Hz, the left ordinate shows the degree of porosity and the right ordinate shows the degree of compaction. With regard to the degree of compaction an increasing trend can be seen over rising frequencies. In addition to Figure 3b, Table 2 contains the different mean values and standard deviations for the change of width and thickness of the consolidated tape which are necessary to calculate the degree of compaction according to Equation (1). With increasing frequencies, the origin width of 11.5 mm raises at 1000 Hz by approx. 4% to 12 mm.

Table 2. Experimental results for compaction and porosity.

Specimen	Thickness μm	Width μm	CSA μm^2	Compaction %	Porosity %
Reference	286 ± 1.91	$11,754 \pm 130$	$3,362,090 \pm 28,536$	8.64 ± 0.78	0.60 ± 0.21
F1	284 ± 2.96	$11,655 \pm 60$	$3,314,010 \pm 32,631$	9.95 ± 0.89	0.38 ± 0.13
F2	276 ± 4.13	$11,785 \pm 113$	$3,279,507 \pm 39,776$	10.88 ± 1.08	0.23 ± 0.09
F3	268 ± 4.28	$12,007 \pm 117$	$3,220,322 \pm 37,621$	12.49 ± 1.02	0.13 ± 0.11

In contrast to the expansion in width, the origin specimen thickness (320 μm) shows a linear decrease over increasing frequency. In reference experiments the thickness decreases by 10.63% to 286 μm , at an excitation frequency of 500 Hz by 13.75% to 276 μm and at a frequency of 1000 Hz by 16.25% to 268 μm . The LSM micrographs with 240 \times magnification (Figure 4) show representatively consolidated specimens. According to calculation of the degree of compaction utilizing Equation (1), an increasing degree of compaction is observable. The compaction increases from 8.64% in the reference experiment to 10.88% in the 500-Hz experiment and 12.49% in the 1000-Hz experiment. The higher degree of compaction is a result of the change in viscosity and the long consolidation time. The compaction of the material only affects the thermoplastic matrix material so that a higher fiber volume content shall be the consequence of this finding.

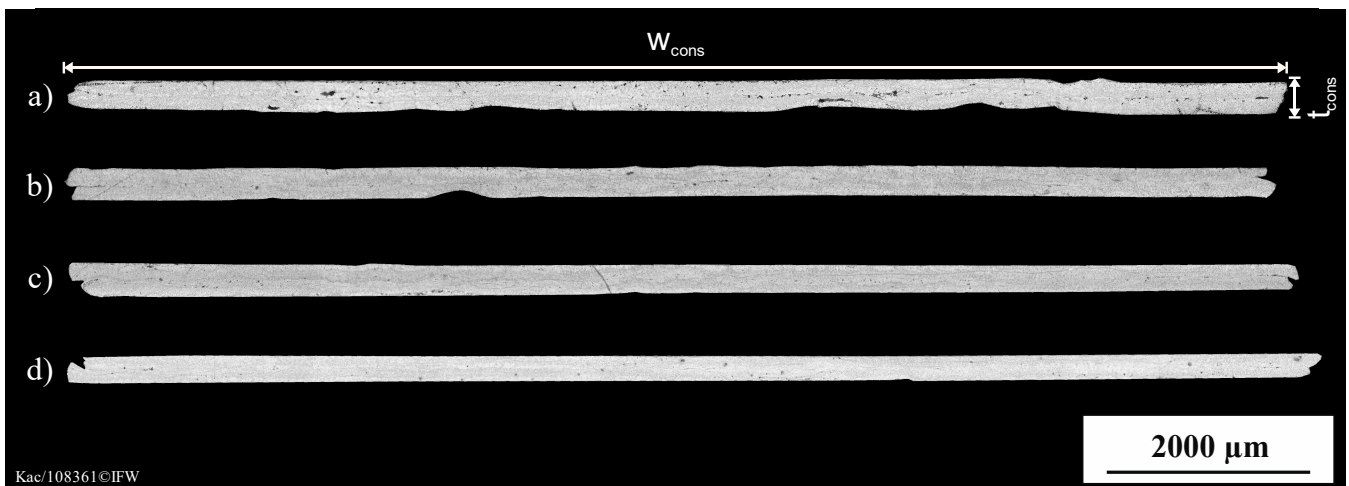


Figure 4. Representative Laser Scanning Microscopy ($240\times$ magnification, stitched) of the cross-sectional area of the manufactured carbon-fiber reinforced polyetheretherketon (PEEK/CF) specimens. (a) Reference experiment. (b) F1 experiment. (c) F2 experiment. (d) F3 experiment.

The LSM micrographs with $1200\times$ magnification (Figure 5) exemplarily show the decrease in the number and size of interlaminar pores which is a consequence of the change in viscosity according to well-known intimate contact models. Additionally, in Figure 3b a decreasing trend in the degree of porosity over increasing frequencies is observable. The pore content reduces from a mean value of 0.6% in the reference experiment to 0.38% in the 100 Hz-experiment. The experiments with higher frequencies also show a decrease in porosities from 0.23% in the 500-Hz experiment to 0.13% in the 1000-Hz experiment. The standard deviation of the determined values is high with regard to the absolute value which agrees with the expectation that the effect is only small due to both the change in viscosity and consolidation pressure. Compared to porosity values obtained in other research on the topic of laser-based in situ TAFP, the porosity values obtained in this work are generally very low. As can be seen in Table 3 the porosity values for PEEK/CF laminates manufactured utilizing laser-based TAFP are between 2 and 4.5%. Since the development of intimate contact and thus the development of interlaminar porosity is time-dependent [9–13] the low porosity values are caused by the consolidation time of 3 s which is quite long compared to typical TAFP consolidation times.

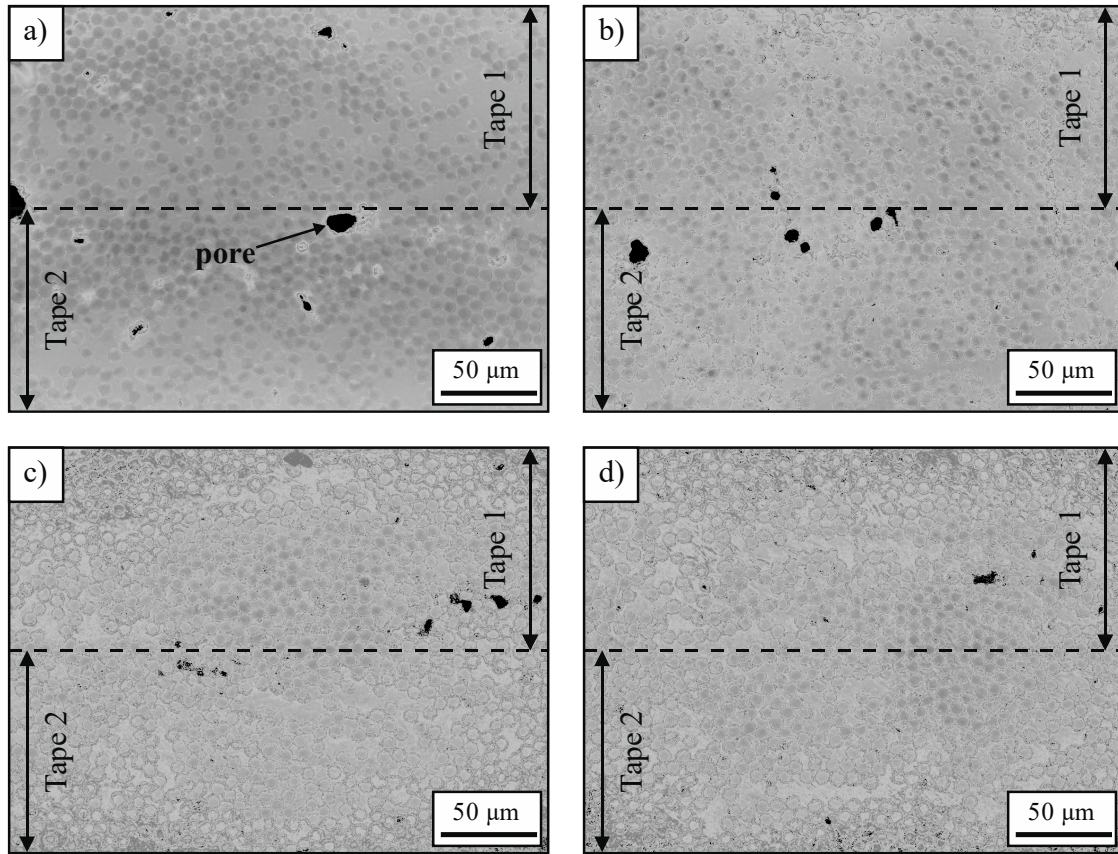
Table 3. Porosity level of PEEK/CF specimens manufactured by laser-based TAFP.

Literature	Material	Placement Velocity	Porosity
[7]	PEEK/CF	8 m/min	$\approx 2.80\%$
[39]	PEEK/CF	12–48 m/min	$\approx 0.80\text{--}4.50\%$
[40]	PEEK/CF	2 m/min	$\approx 3.00\%$

3.3. Degree of Crystallization

To evaluate the influence of vibrations on recrystallization of the PEEK material after consolidation, the degree of crystallization was calculated according to Equation (3) for three different vibration-assisted consolidation forces and the reference experiment. The reference sample had not been exposed to vibration during consolidation; the other samples were consolidated with a frequency of 100 Hz, 500 Hz and 1000 Hz. In Figure 6, for all the different samples the melting peak of the first heating cycle is shown. It is observable that the curves are nearly congruent. All the curves have no recrystallization peak, which means that the cooling rate during consolidation is slower than 15 K/s. The degree of crystallization amounts by the reference sample 38%, which is the highest degree of crystallization of the four samples. In contrast, the lowest degree of crystallization is reached by a frequency of 100 Hz and amounts

to 32%. The samples which were consolidated with a frequency of 500 Hz and 1000 Hz have a degree of crystallization of 35%. At the second heating cycle all samples have also nearly the same degree of crystallization of about 35%, thus it was shown that the vibrations do not damage the polymer chains. The DSC experiments also show that the frequency has no remarkable influence in the crystallization process.



Kac/108362©IFW

Figure 5. Representative Laser Scanning Microscopy (1200× magnification, height thresholded) of the cross-sectional area of the boundary interface of the PEEK/CF specimens. (a) Reference experiment. (b) F1 experiment. (c) F2 experiment. (d) F3 experiment.

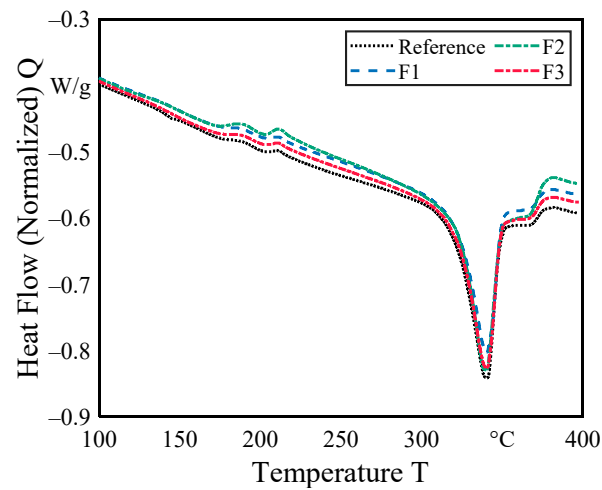


Figure 6. Differential Scanning Calorimetry curves for the manufactured double-layer PEEK/CF specimens.

4. Discussion and Conclusions

In this work, an approach for improving consolidation quality within a pre-heated in situ consolidation process by applying sub-ultrasonic vibrations is experimentally investigated. Preliminary experimental investigations of the vibration-excited consolidation were carried out using a simplified test setup within a universal testing machine. The consolidation of two PEEK/CF tapes has shown that there are several effects following the excitation frequency to improve the bonding quality. Using optical (LSM) and thermal (DSC) methods, the interlaminar pore content, the degree of compaction and the degree of crystallization were determined to evaluate the influence of sub-ultrasonic vibrations on the consolidation quality. The key findings of these experimental studies carried out are:

- The static consolidation force has a higher decreasing rate for higher frequencies which leads to the conclusion that the relaxation capacity of the viscoelastic PEEK material increases. This is due to a decrease in viscosity, which is beneficial for the development of intimate contact. However, for use in AFP systems a fast pressure control system has to be implemented to control the reduced pressure according to the lay-up velocity.
- Considering the consolidation force results, it was found that the interlaminar pore content can be reduced in the consolidation of PEEK/CF tapes by applying high frequencies (>500 Hz) during the consolidation process. A positive consequence is a higher degree of intimate contact. Due to the high consolidation time the absolute values of porosity are very low and thus not representative for TAFP processes.
- The degree of compaction increases with increasing frequency. An increase in width and a decrease in thickness can be seen here.

Since the intimate contact, and thus porosity and compaction, are time-dependent effects and the consolidation time in this work is long compared to the AFP time, further investigations will be conducted with regard to different consolidation times. In order to study the dependencies of applied vibration and consolidation time, respectively placement velocity, a novel sub-ultrasonic vibration-assisted consolidation roller will be utilized within laser-based AFP. In addition, the mechanical properties of consolidation specimens are not investigated in this work. Therefore, future work will also include mechanical testing of AFP manufactured specimens to evaluate the bond strength, in addition to the microscopic examination of the bonding interface, to obtain holistic knowledge about the sub-ultrasonic vibration-assisted consolidation.

Author Contributions: Conceptualization, C.S., M.K. and M.S.; formal analysis, M.K. and M.S.; funding acquisition, B.D. and C.S.; investigation, M.K. and M.S.; methodology, C.S. and M.K.; project administration, B.D. and C.S.; supervision, B.D. and C.S.; validation, M.K. and M.S.; visualization, M.K.; writing—original draft, M.K. and M.S.; writing—review and editing, B.D. and C.S. All authors have read and agreed to the published version of the manuscript.

Funding: The authors thankfully acknowledge the financial and organizational support of the project Join THIS by the federal state of Lower Saxony and the European Regional Development Fund (ERDF). The publication of this article was funded by the Open Access Fund of the Leibniz Universität Hannover.

Data Availability Statement: The data presented in this study are available on request from the corresponding author.

Conflicts of Interest: The authors declare no conflict of interest.

References

1. Schledjewski, R. Thermoplastic tape placement process—In situ consolidation is reachable. *Plast. Rubber Compos.* **2009**, *38*, 379–386. [[CrossRef](#)]
2. Stokes-Griffin, C.M.; Matuszyk, T.I.; Compston, P.; Cardew-Hall, M.J. Modelling the Automated Tape Placement of Thermoplastic Composites with In-Situ Consolidation. In *Sustainable Automotive Technologies, Proceedings of the 4th International Conference, Melbourne, Australia; Subic, Wellnitz, Leary, Koopmans*; Springer: Heidelberg, Germany, 2012. [[CrossRef](#)]
3. Dara, P.H.; Loos, A.C. *Thermoplastic Matrix Composite Processing Model*; Virginia Polytechnic Institut: Blacksburg, VA, USA, 1985.

4. Stokes-Griffin, C.M.; Compston, P.; Matuszyk, T.I.; Cardew-Hall, M.J. Thermal modelling of the laser-assisted thermoplastic tape placement process. *J. Thermoplast. Compos. Mater.* **2015**, *28*, 1445–1462. [[CrossRef](#)]
5. Sarrazin, H.; Springer, G.S. Thermochemical and mechanical aspects of composite tape laying. *J. Compos. Mater.* **1995**, *29*, 1908–1943. [[CrossRef](#)]
6. Maurer, D.; Mitschang, P. Laser-powered tape placement process-simulation and optimization. *Adv. Manuf. Polym. Compos. Sci.* **2015**, *1*, 129–137. [[CrossRef](#)]
7. Comer, A.J.; Ray, D.; Obande, W.O.; Jones, D.; Lyons, J.; Rosca, I.; O'Higgins, R.M.; McCarthy, M.A. Mechanical characterization of carbon fibre-PEEK manufactured by laser-assisted automated-tape-placement and autoclave. *Compos. Part A Appl. Sci. Manuf.* **2015**, *69*, 10–20. [[CrossRef](#)]
8. Groupe, W.J.B.; Warnet, L.L.; Rietmann, B.; Akkerman, R. On the weld strength of in situ tape placed reinforcements on weave reinforced structures. *Compos. Part A Appl. Sci. Manuf.* **2012**, *43*, 1530–1536. [[CrossRef](#)]
9. Lee, W.I.; Springer, G.S. A Model of the Manufacturing Process of Thermoplastic Matrix Composites. *J. Compos. Mater.* **1987**, *21*, 1017–1055. [[CrossRef](#)]
10. Pitchumani, R.; Ranganathan, S.; Don, R.C.; Gillespie, J.W.; Lamontia, M.A. Analysis of transport phenomena governing interfacial bonding and void dynamics during thermoplastic tow-placement. *Int. J. Heat Mass. Transf.* **1996**, *39*, 1883–1897. [[CrossRef](#)]
11. Pitchumani, R.; Gillespie, J.W.; Lamontia, M.A. Design and Optimization of a Thermoplastic Tow-Placement Process with in-situ Consolidation. *J. Compos. Mater.* **1997**, *31*, 244–275. [[CrossRef](#)]
12. Yang, F.; Pitchumani, R. A fractal Cantor set based description of interlaminar contact evolution during thermoplastic composites processing. *J. Mater. Sci.* **2001**, *36*, 4461–4671. [[CrossRef](#)]
13. Yang, F.; Pitchumani, R. Nonisothermal Healing and Interlaminar Bond Strength Evolution During Thermoplastic Matrix Composites Processing. *Polym. Compos.* **2003**, *24*, 263–278. [[CrossRef](#)]
14. Khan, M.A.; Mitschang, P.; Schledjewski, R. Identification of some optimal parameters to achieve higher laminate quality through tape placement process. *Adv. Polym. Technol.* **2010**, *29*, 98–111. [[CrossRef](#)]
15. Celik, O.; Peeters, D.; Dransfeld, C.; Teuwen, J. Intimate contact development during laser assisted fiber placement: Microstructure and effect of process parameters. *Compos. Part A Appl. Sci. Manuf.* **2020**, *134*. [[CrossRef](#)]
16. Oromiehie, E.; Garbe, U.; Prusty, B.G. Porosity analysis of carbon fibre-reinforced polymer laminates manufactured using automated fibre placement. *J. Compos. Mater.* **2020**, *54*, 1217–1231. [[CrossRef](#)]
17. Leon, A.; Argerich, C.; Barasinski, A.; Soccard, E.; Chinesta, F. Effects of material and process parameters on in-situ consolidation. *Int. J. Mater. Form.* **2019**, *12*, 491–503. [[CrossRef](#)]
18. Stokes-Griffin, C.M.; Compston, P. Investigation of sub-melt temperature bonding of carbon-fibre/PEEK in an automated laser tape placement process. *Compos. Part A Appl. Sci. Manuf.* **2016**, *84*, 17–25. [[CrossRef](#)]
19. Stokes-Griffin, C.M.; Compston, P. An inverse model for optimization of laser heat flux distributions in an automated laser tape placement process for carbon-fibre/PEEK. *Compos. Part A Appl. Sci. Manuf.* **2016**, *88*, 190–197. [[CrossRef](#)]
20. Schaefer, P.M.; Guglhoer, T.; Sause, M.G.R.; Drechsler, K. Development of intimate contact during processing of carbon fiber reinforced Polyamide-6 tapes. *J. Reinf. Plast. Compos.* **2017**, *36*, 593–607. [[CrossRef](#)]
21. Celik, O.; Teuwen, J. Effects of Process Parameters on Intimate Contact Development in Laser Assisted Fiber Placement. In Proceedings of the 4th Automated Composites Manufacturing (ACM4), Montreal, QC, Canada, 25–26 April 2019.
22. Levy, A.; Heider, D.; Tierney, J.; Gillespie, J.W. Inter-layer thermal contact resistance evolution with the degree of intimate contact in the processing of thermoplastic composite laminates. *J. Compos. Mater.* **2014**, *48*, 491–503. [[CrossRef](#)]
23. Stokes-Griffin, C.M.; Compston, P.; Stokes-Griffin, C.M.; Compston, P. A combined optical-thermal model for near-infrared laser heating of thermoplastic composites in an automated tape placement process. *Compos. Part A Appl. Sci. Manuf.* **2015**, *75*, 104–115. [[CrossRef](#)]
24. Stokes-Griffin, C.M.; Compston, P. The effect of processing temperature and placement rate on the short beam strength of carbon fibre-PEEK manufactured using a laser tape placement process. *Compos. Part A Appl. Sci. Manuf.* **2015**, *78*, 274–283. [[CrossRef](#)]
25. Barasinski, A.; Leygue, A.; Soccard, E.; Poitou, A. In situ consolidation for thermoplastic tape placement process is not obvious. *AIP Conf. Proc.* **2011**, *1353*, 948. [[CrossRef](#)]
26. Kok, T.; Groupe, W.J.B.; Warnet, L.L.; Akkerman, R. Intimate contact development in laser assisted fiber placement. In Proceedings of the ECCM17—17th European Conference on Composite Materials, Munich, Germany, 26–30 June 2016; Drechsler. ESCM European Society for Composite Materials: Munich, Germany, 2016.
27. Sonmez, F.O.; Akbulut, M. Process optimization of tape placement for thermoplastic composites. *Compos. Part A Appl. Sci. Manuf.* **2007**, *38*, 2013–2023. [[CrossRef](#)]
28. Kollmansberger, A. Heating Characteristics of Fixed Focus Laser Assisted Thermoplastic-Automated Fiber Placement of 2D and 3D Parts. Ph.D. Thesis, Technical University Munich, Munich, Germany, 2019.
29. Brzeski, M. Experimental and Analytical Investigation of Deconsolidation for Fiber Reinforced Thermoplastic Composites. Ph.D. Thesis, Technical University Kaiserslautern, Kaiserslautern, Germany, 2014.
30. Lionetto, F.; Dell'Anna, R.; Montagna, F.; Maffezzoli, A. Modeling of continuous ultrasonic impregnation and consolidation of thermoplastic matrix composites. *Compos. Part A Appl. Sci. Manuf.* **2016**, *82*, 119–129. [[CrossRef](#)]
31. Rizzolo, R.H.; Walczyk, D.F. Ultrasonic consolidation of thermoplastic composite prepreg for automated fiber placement. *J. Thermoplast. Compos. Mater.* **2016**, *29*, 1480–1497. [[CrossRef](#)]

32. Chu, Q.; Li, Y.; Xiao, J.; Huan, D.; Zhang, X.; Chen, X. Processing and characterization of the thermoplastic composites manufactured by ultrasonic vibration-assisted automated fiber placement. *J. Thermoplast. Compos. Mater.* **2018**, *31*, 339–358. [[CrossRef](#)]
33. Tolunay, M.N.; Dawson, P.R. Heating and Bonding Mechanisms in Ultrasonic Welding of Thermoplastics. *Polym. Eng. Sci.* **1983**, *23*, 726–733. [[CrossRef](#)]
34. Benatar, A.; Gutowski, T.G. Ultrasonic Welding of PEEK Graphite APC-2 Composites. *Polym. Eng. Sci.* **1989**, *29*, 1705–1721. [[CrossRef](#)]
35. Levy, A.; Le Corre, S.; Villegas, I.F. Modeling of the heating phenomena in ultrasonic welding of thermoplastic composites with flat energy directors. *J. Mater. Process. Technol.* **2014**, *214*, 1361–1371. [[CrossRef](#)]
36. Jeng, C.; Chen, M. Flexural failure mechanisms in injection-moulded carbon fibre/PEEK composites. *Compos. Sci. Technol.* **2000**, *60*, 1863–1872. [[CrossRef](#)]
37. Mantell, S.C.; Springer, G.S. Manufacturing Process Models for Thermoplastic Composites. *J. Compos. Mater.* **1992**, *29*, 2348–2377. [[CrossRef](#)]
38. Khan, M.A.; Mitschang, P.; Schledjewski, R. Parametric study on processing parameters and resulting part quality through thermoplastic tape placement process. *J. Compos. Mater.* **2013**, *47*, 485–499. [[CrossRef](#)]
39. Di Francesco, M.; Giddings, P.F.; Scott, M.; Goodman, E.; Dell'Anno, G. Influence of laser power density on the meso-structure of thermoplastic composite preforms manufactured by automated fibre placement. In *International SAMPE Technical Conference, Proceedings of the SAMPE Long Beach 2016 Conference and Exhibition, Long Beach, CA, USA, 23–26 May 2016*; Society for the Advancement of Material and Process Engineering: Diamond Bar, CA, USA, 2016.
40. Saenz-Castillo, D.; Martin, M.I.; Garcia-Martinez, V.; Ramesh, A.; Battley, M.; Güemes, A. A comparison of mechanical properties and X-ray tomography analysis of different out-of-autoclave manufactured thermoplastic composites. *J. Reinf. Plast. Compos.* **2020**, *39*, 703–720. [[CrossRef](#)]